Dynamics of an electronic relay systems with bandpass filtered feedback

Lucas Illing[1], Kees Benkendorfer[1,2], Pierce Ryan[3], and Andreas Amann[3]

[1] Department of Physics, Reed College, Portland, Oregon, 97202, USA (E-mail: illing@reed.edu)
[2] Laboratory for Particle Physics and Cosmology, Harvard University, Cambridge, MA, USA
[3] School of Mathematical Sciences, University College Cork, Cork T12 XF62, Ireland

Abstract. Delay dynamics have wide relevance in fundamental science and technology due to the ubiquitous presence of feedback loops in which time lags arise because of natural processes, control interfaces, or performance limits of components. We present results from a well-controlled experiment that is representative of feedback systems with relays (switches) that actuate after a fixed delay. Notably, the system exhibits strong multirhythmicity, the coexistence of many stable periodic solutions for the same values of parameters. We then study the system dynamics analytically. The model we consider is a nonsmooth second-order delay differential equation that describes single-input single-output systems in which the delayed feedback is a bandpass filtered relay signal. We discuss how periodic solutions and bifurcations can be obtained by reducing the system to a set of finite-dimensional maps. We find good agreement between theory and experiment.
Keywords: Nonlinear dynamics, Bifurcations, Delay differential equations, Nonlinear circuits, Relay systems, Nonsmooth dynamical systems, Quasiperiodic oscillations.

1 Introduction

In this paper we study the dynamics of a time-delayed relay systems.

A relay refers to a switch that flips between two or more fixed outputs depending on its input. Relay models of naturally occurring systems arise when nonlinearities are well approximated by functions that take on discrete values [1, 2]. Relays also have great practical importance in man-made systems because relay feedback control systems are applied in many different areas of engineering. In this paper we consider relays that switch between two constant outputs without hysteresis and, consequently, model the relay nonlinearity as

$$\operatorname{sign}(x) = \begin{cases} +1 & x \geq 0 \\ -1 & x < 0 \end{cases}. \tag{1}$$

16^{th} *CHAOS Conference Proceedings, 13-16 June 2023, Heraklion, Crete, Greece*

Delay arises naturally due to finite signal transmission and processing times, sampling delays, or latencies in external control loops. The addition of such delay terms to a differential equation describing the system evolution generally introduces a wealth of complex dynamic behavior on multiple time scales [2–10]. If delay arises in relay systems, the model becomes a nonsmooth delay differential equation (DDE). Due to their importance, nonsmooth DDEs have been the focus of much recent attention [1, 2, 11–15].

First order DDEs of relay systems are well understood. In first order DDEs with a negative delayed relay feedback, one typically finds that there is a unique nonasymptotically (orbitally) stable slowly oscillating periodic solution [11, 12, 16–18].† This can be shown rigorously if the first order DDE is linear (aside from the relay term) and also holds for nonlinear DDEs under certain boundedness assumptions [11, 12]. In such systems, there exists a countably infinite set of rapidly oscillating periodic solutions, but all of these are unstable. Therefore, in practice, such systems converge to the slowly oscillating solution [18].

Compared to first order systems, the dynamics of second order time-delayed relay systems is less well understood. Yet, second order DDEs are often required to accurately describe natural phenomena and technological applications. Therefore, we study in this paper one of the simplest second order models, a linear second order time-delayed relay system in which velocity serves as the feedback signal. We show in experiment and theory that the system exhibits strong *multirhythmicity*, the coexistence of multiple stable periodic solutions [19].

2 Multirhythmicity

The coexistence of many periodic solutions is a common feature of DDEs. This is seen by considering, as an example, a periodic solution $x(t)$ of a scalar DDE $\dot{x} = F[x(t), x(t-\tau)]$ that has a period p and ν zero crossings of x per delay interval τ. The periodic function x is also a solution to the same DDE with the delay increased to $\tau' = \tau + n\,p$ ($n = 1, 2, 3, \ldots$), since the right hand side of the DDE is left invariant. With regard to the new delay τ', the solution has a larger number of zero crossings per delay ($\nu' > \nu$).

If one considers now smooth changes of the delay parameter τ' back to τ and assumes that the solution x deforms but continues to exist as a solution with ν'-zero crossings, then the DDE must have periodic solutions with both ν and ν' crossings. The existence of a single periodic solution would then imply an infinite number of coexisting periodic solutions (since n is arbitrary). Of course, the assumption in this argument can break down, such as for solutions that are destroyed by bifurcations upon variation of τ. It is therefore necessary to study solutions and their domain of existence in detail.

† Slowly oscillating refers to periodic solutions with period larger than twice the delay, whereas solutions with periods less than twice the delay are said to be rapidly oscillating.

Furthermore, the argument says nothing about stability and it is exactly the question of stability that we are interested in. While there are, typically, no coexisting stable periodic solutions for linear first order delayed relay systems (only the slowly oscillating solution is stable), coexisting stable solutions do exist for linear second order delayed relay systems. To demonstrate this multirhythmicity, we first discuss an experiment demonstrating this fact and then explain how the linear second order delayed relay model describing the experiment can be reduced to a set of maps that allow one to establish multirhythmicity analytically.

3 Multirhythmicity in Experiment

In our experiment, an external function generator is used to write an initial waveform into the feedback loop, as shown in the schematic in Fig. 1. After the initial history function is written, the switch is actuated, thereby disconnecting the function generator, closing the feedback loop, and making the system autonomous. In the feedback loop of the autonomous system, the output of the bandpass filter (V_{out}), passes through a relay nonlinearity, the output of which is attenuated and serves as the input (IN) of a programmable electronic delay. The delayed signal (OUT) is amplified and provides the input to the bandpass filter, closing the loop.

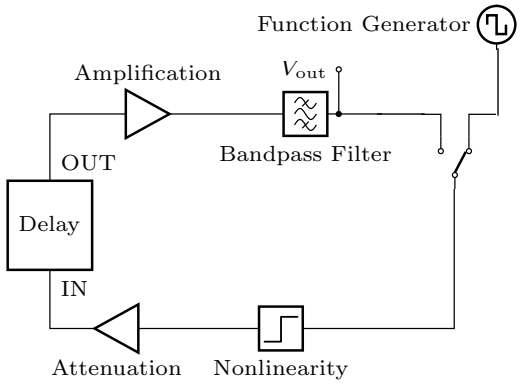

Fig. 1. Schematic representation of experiment.

The experiment is well modeled by a simple linear second-order DDE with a relay nonlinearity, which is obtained as follows: We define the input of the bandpass filter as V_{in}. Then, the action of the relay nonlinearity, attenuator, delay, and amplifier can be written as

$$V_{\text{in}}(t) = f\left[V_{\text{out}}(t-\tau)\right], \tag{2}$$

with

$$f\left[V_{\rm out}(t-\tau)\right] = \begin{cases} \gamma V_s & V_{\rm out}(t-\tau) \geq 0 \\ -\gamma V_s & V_{\rm out}(t-\tau) < 0 \end{cases}, \tag{3}$$

where $V_s = 15\,\mathrm{V}$ is a fixed rail voltage and γ is the combined gain of the attenuator, delay, and amplifier (see App. A for a details).

As shown in App. A, the action of the bandpass filter is described by the integro-differential equation

$$V_{\rm out}(t) + \frac{Q}{\omega_c}\,\dot{V}_{\rm out}(t) + Q\,\omega_c \int^t V_{\rm out}(s)\,\mathrm{d}s = -G\,f\left[V_{\rm out}(t-\tau)\right], \tag{4}$$

where G is the filter's gain, Q its quality factor, ω_c its center angular frequency, and we made use Eq. (2) to replace $V_{\rm in}$. The introduction of the dimensionless variable

$$y = \frac{Q\,\omega_c}{\gamma\,G\,V_s} \int^t V_{\rm out}(s)\,\mathrm{d}s \tag{5}$$

maps Eq. (4) onto the nonsmooth DDE

$$\omega_c^{-2}\,\ddot{y} + (\omega_c\,Q)^{-1}\,\dot{y} + y = -\mathrm{sign}[\dot{y}(t-\tau)]. \tag{6}$$

This is the second-order nonsmooth DDE whose nontrivial dynamics we are exploring.

To demonstrate multirhythmicity, i.e. the coexistence of stable slow and fast-oscillating solutions, one needs to initialize the system in the basin of attraction of the desired stable periodic orbit. To do so, a $\pm 10\,\mathrm{V}$ square wave at a particular frequency was generated by the function generator and fed to the system through the switch. The system was then transitioned into feedback mode by throwing the switch. The switching action was fast enough such that the voltage history in the feedback loop would result in system oscillations at the driving frequency for times immediately following the switching. Thus, the circuit could be perturbed into a region of interest in frequency-space.

At a given delay, the system was pushed into varying regions of frequency space, starting around the slow-oscillatory solution, within and around the passband of the bandpass filter. After each initialization, the circuit was allowed to settle into a stable oscillatory solution, the period of which was subsequently recorded. This was repeated with increasing initial frequencies until no new final periods were found and the system consistently decayed to already observed asymptotic solutions.

The result of this procedure for a fixed delay τ and fixed bandpass filter is displayed in Fig. 2. It is seen that there are four coexisiting stable asymptotic solutions with inverse period of $105.5\,\mathrm{s}^{-1}$, $314.6\,\mathrm{s}^{-1}$, $523.5\,\mathrm{s}^{-1}$, and $733\,\mathrm{s}^{-1}$, respectively. Initial square waves with frequencies close to the frequency of one of the asymptotic solutions were found to decay to it, as seen by the corresponding colors in Fig. 2. Initial square waves with frequencies well above those of the four asymptotic solutions tended to decay to one of the lower frequency

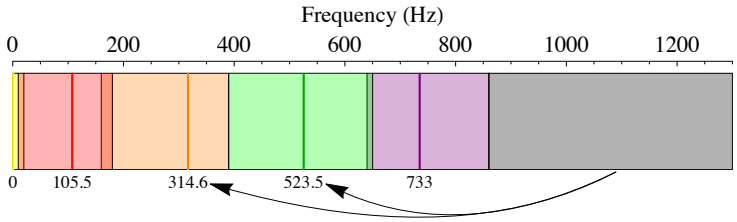

Fig. 2. Frequencies of driven initial oscillations and the inverse period of the solution to which they decayed (dark lines) during trial 1 (see Tab. 1) with a delay of $\tau = 4.765(3)\,\mathrm{ms}$. Colored bars represent the basins of attraction of the asymptotic oscillatory solutions of the same color within them. Above an initial frequency of 860 Hz (grey bar), the system jumped over the $733\,\mathrm{s}^{-1}$ solution and decayed to lower frequency solutions.

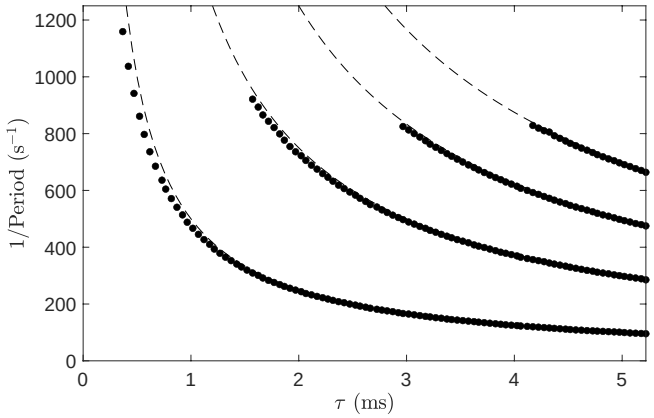

Fig. 3. Diagram of observed inverse periods of the stable attracting asymptotic oscillations (black circles) for delays between 0.515(3) ms and 5.265(3) ms and bandpass parameters of trial 1 (see Tab. 1). The dashed lines are functions of the form $n/(2\tau)$ for $n \in \{1, 3, 5, 7\}$.

solutions, skipping the $733\,\mathrm{s}^{-1}$ stable solution. This can be interpreted as an indication that the basin of attraction of the $733\,\mathrm{s}^{-1}$ stable solution is smaller than the other basins.

In Fig. 3 we show, for a fixed bandpass filter, the inverse period of the asymptotic solutions as a function of the delay τ. As indicated by the dashed lines, the period of the modes is roughly equal to 2τ divided by an odd number (odd due to the use of negative feeback). It is seen that the number of stable coexisting solutions increases as the delay is increased, up to four solutions at $\tau = 5\,\mathrm{ms}$. Thus, the bandpass filtered relay circuit clearly demonstrates strong multirhythmicity in the limit of large delays.

To explore the effect of the bandpass filter on the number of periodic solutions (modes), we varied the corner frequencies. Narrowing the passband by lowering the upper 3 dB frequency from 3.4 kHz, to 1.6 kHz, to 0.8 kHz did reduce the number of coexisting modes. For example, at a delay of $\tau = 5\,\mathrm{ms}$

from 9 to 5 to 3 modes. In contrast, narrowing the passband by increasing the lower 3 dB frequency from 24 Hz, to 48 Hz, to 91 Hz did not decrease the number of stable modes. This is shown in Fig. 4, which demonstrates that at $\tau = 5$ ms the number of modes actually increased from 4 to 5.

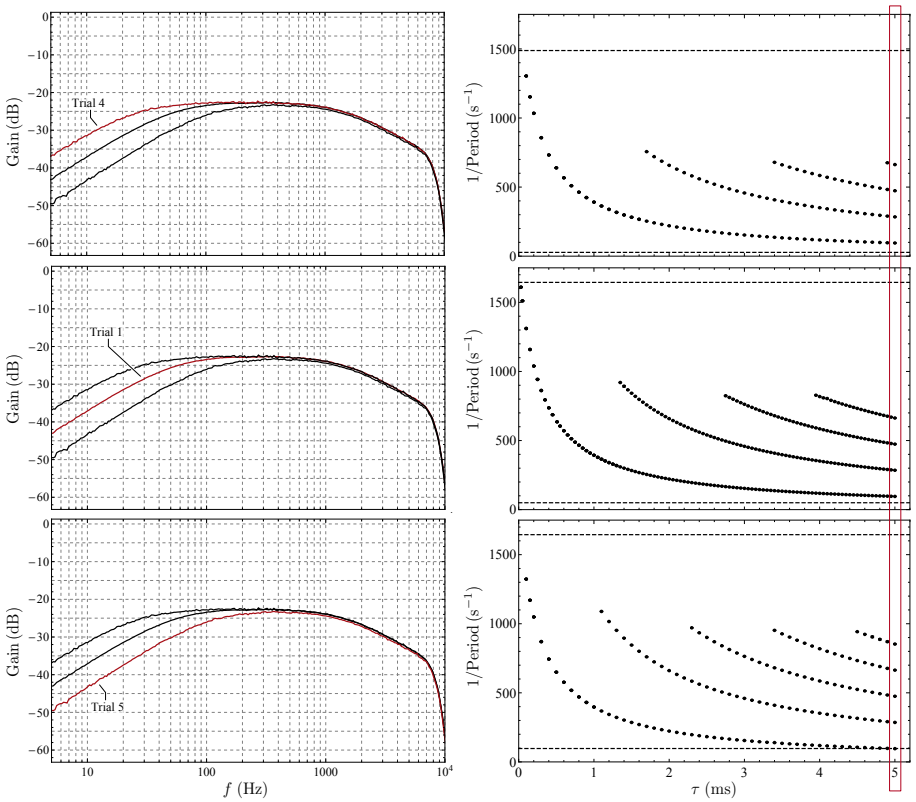

Fig. 4. Narrowing the passband by raising the lower 3dB corner frequency: Transfer function magnitude (gain vs frequency) of the circuit with the relay circuit element removed (left column, top to bottom: trial 4, 1, 5 [see Tab. 1]) alongside experimentally determined modes (right column). The bottom and top dashed lines show the lower corner frequency and the upper corner frequency, respectively.

It is interesting, and somewhat counterintuitive, that narrowing of the passband does not necessarily lead to a decrease in the number of stable modes. We will now turn to an analytic treatment to show how this result corresponds to theory.

4 Multirhythmicity in Theory

In order to solve the delayed relay system DDE (6), we note that it is sufficient to keep track of the headpoint coordinates $(y(t), \dot{y}(t))$ and the sign of $\dot{y}$ in

the delay interval or, equivalently, the times τ_n at which $\dot{y}$ crosses zero with $t - \tau < \tau_k < \tau_{k-1} < \ldots < \tau_1 \leq t$. The state of the system at time t is a tuple of variable length $k + 2$,

$$S(t) = (y, \dot{y}; \tau_1, \tau_2, \ldots, \tau_k). \tag{7}$$

The solution can be obtained in terms of a discrete time map acting on S that maps between key events. There are two key events that affect $S(t)$:

1. A *zero* element is added at time $t = t_n$. When $\dot{y}$ passes through zero, a zero element equal to t_n is added to S; this does not immediately cause the relay feedback to change but it will switch the sign of the feedback at time $t_n + \tau$. Such an event is denoted by the symbol Z if $\dot{y}$ transitions from negative to positive and by $\overline{Z}$ for the opposite transition.
2. A zero-crossing time is removed from the *history*. When $\tau_k(t) = t - \tau$, τ_k is deleted from S. The sign of the relay feedback switches. Such an event is denoted by the symbol H if the feedback switch is due to a transition of $\dot{y}(t - \tau)$ from negative to positive and by $\overline{H}$ for the opposite transition.

Between consecutive events, the feedback term in DDE (6) is constant, either $+1$ or -1. The evolution is given by the solution of a linear ordinary differential equation. Explicit solution of the ODE allows us to construct an iterative map that moves the system forward in time from one event to the next.

Every oscillatory solution thereby generates a symbolic-sequence of events, with periodic solutions represented by repeated sequences. We find that periodic orbits of interest are those that have a repeating sequence of four events per period, either $[H, \overline{Z}, \overline{H}, Z]$ or $[H, Z, \overline{H}, \overline{Z}]$, where we start all sequences with H for consistency (every cyclic permutation of a repeating sequence represents the same solution).

As detailed in [20], one can construct explicitly Poincaré maps that advance solutions forward by four symbols. The fixed points of these maps are the desired periodic solutions. We recall that the state vector in Eq. (7) has a size that is given in terms of the integer k. Accordingly, there is a separate Poincaré map for each integer k. In addition to obtaining the unique Poincaré-map fixed point for each k, the linear stability analysis of these solutions has been carried out explicitly [20], thereby analytically determining the stability of the periodic solutions.

When discussing the dynamics of DDE (6), it is useful to distinguish the underdamped ($Q > 1/2$) and overdamped ($0 < Q < 1/2$) regime. In the underdamped regime, the transient response of the filter due to nonzero initial conditions is oscillatory, whereas it is nonoscillatory in the overdamped regime. In the overdamped regime, all stable solutions found in our analysis were periodic and all bifurcations were smooth standard bifurcations, whereas a much richer solution and bifurcation structure exists in the underdamped regime [20]. Both regimes display multirhythmicity. In this paper we focus exclusively on the overdamped regime because the experiments were conducted with $Q < 1/2$.

The DDE (6) depends on just two dimensionless parameters, the quality factor Q and the dimensionless parameter $\Omega = \omega_c \tau$, the product of the filter

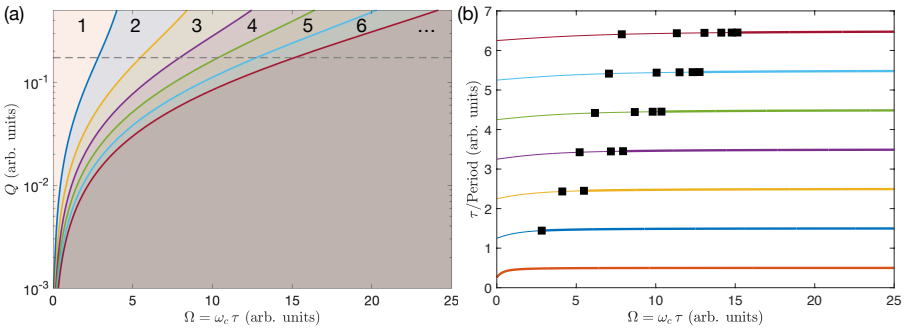

Fig. 5. (a) Stable periodic oscillations in the overdamped regime (colored regions, overlapping), stabilizing Neimarck-Sacker bifurcations (solid colored lines), and number of coexisting stable periodic solutions. (b) Scaled inverse period versus Ω of first seven modes for $Q = 0.1731$ (gray dashed line in a). Mode stability: unstable (thin line), stable (thick line). Bifurcations: Neimarck-Sacker bifurcations (solid squares).

center frequency and the delay. In terms of these parameters, a summary of the periodic solutions and bifurcations in the overdamped regime is shown in Fig. 5. The first seven stable modes are shown in Fig. 5a, each represented by a color, and the stabilizing Neimarck-Sacker bifurcation (torus bifurcation of the DDE) by a solid line of corresponding color. The number of coexisting modes grows as Ω increases. Once a mode is stabilized, there are no further bifurcations of a mode as Ω is increased further [20]. Thus, the system exhibits strong multirhythmicity; the number of coexisting modes increases without bound in the $\tau \to \infty$ limit.

The period of the modes is approximately proportional to the delay. Therefore, in Fig. 5b, we show the inverse period of the first seven modes scaled by τ. The figure demonstrates the fact that, in the overdamped regime, all modes always coexist. The rapidly oscillating modes are unstable for small τ and are stable above some mode-dependent critical value of τ. The slowly oscillating mode (red lowest curve) is always stable.

To explain the experimentally observed dependence of the number of stable modes on the bandpass filter, we note that, for a fixed delay, narrowing the passband by decreasing the upper 3 dB corner frequency will increase Q and decrease Ω (decrease ω_c). As seen by Fig. 5a, this tends to move the system into a regime with a lower number coexisting stable solutions. In contrast, narrowing the passband by increasing the lower 3 dB corner frequency of the bandpass filter will increase both Q and Ω. This can move the system into a regime with a larger number coexisting stable solutions, in agreement with the experimental results.

5 Comparison of Experiment and Theory

In Fig. 6a we show the data of the experiment in which the filter passband was decreased by increasing the low-frequency cutoff (same as Fig. 4). To compare theory and experiment we then utilize the known quality factor Q and center

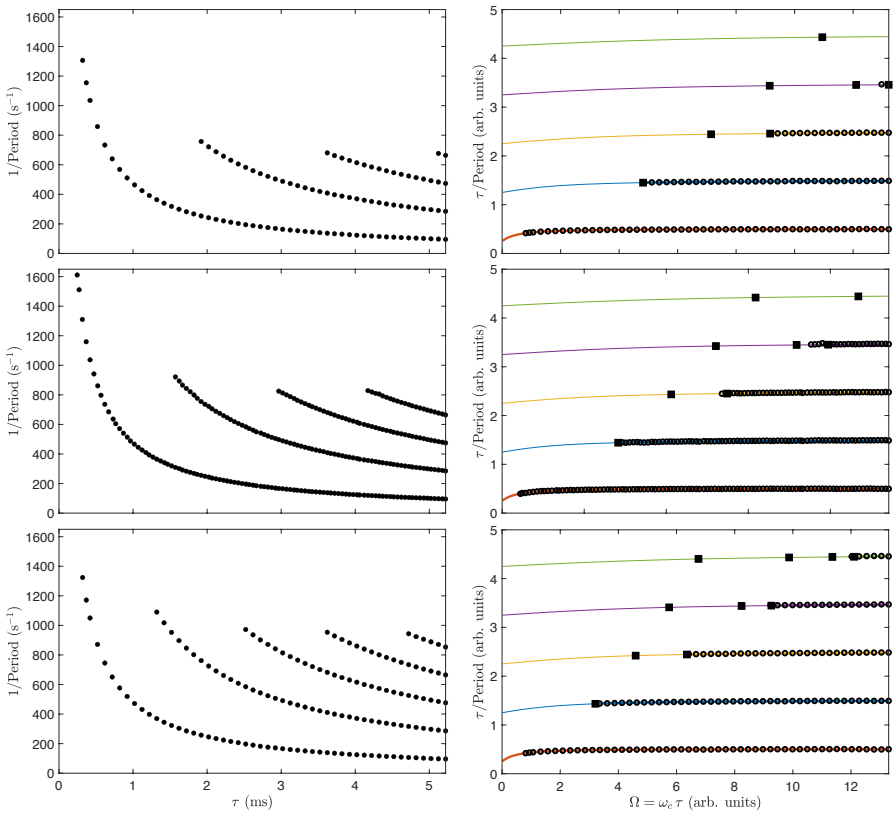

Fig. 6. (Left column) Observed inverse periods of stable attracting asymptotic oscillations (black circles) for delays between 0.515(3) ms and 5.265(3) ms (same data as in Fig. 4). (Right column) Data (black circles) replotted on top of theoretical predictions with unstable (thin line) and stable (thick line) solutions as well as Neimarck-Sacker bifurcations (solid squares) indicated.

frequency ω_c for each choice of corner frequency in order replot this data on top of the theoretical predictions, as shown in Fig. 6b.

It is seen that the measured and predicted periods of the coexisting solutions are in excellent agreement. Furthermore, the regions of stability agree. The slowly oscillation solution (red) is always stable (experimental limitations did not allow us to access delays below ~ 0.5 ms). For rapidly oscillating solutions, it is seen that the theoretically determined value of Ω at which a subcritical Neimark-Sacker bifurcation of the map (subcritical torus bifurcation of the DDE) stabilizes a solution is in excellent agreement with the minimal value of Ω for which the corresponding mode is found in experiment. Small differences for higher frequency modes are due to the fact that the simple two-pole bandpass filter model is an approximation to the actual transfer function.

6 Discussion

This paper advances the study of relay systems. We discuss a model and an experiment that are representative of systems that exhibit harmonic oscillator type dynamics and have a time delayed relay feedback of the velocity signal. They also represent systems with a delayed and bandpass filtered relay-type feedback signal.

The model we consider is the linear second order DDE given by Eq. (6). This paper focuses on negative feedback and the overdamped regime. Under these conditions, the slowly oscillating solution of DDE (6) is always stable, similar to first order delayed relay systems. In contradistinction to first order delayed relay systems, this second-order systems exhibits strong multirhythmicity. That is, many stable rapidly oscillating solutions coexist with the slowly oscillating solution. Nevertheless, the system dynamics are relatively simple. Aside from periodic solutions, no other stable solutions were found in the overdamped regime either numerically or in experiment.

Why is the dynamics of DDE (6) in the overdamped regime so simple? One possible explanation is to note that the ODE flow associated with the DDE gives rise to restrictions. That is, after an instant in which the delayed feedback switches sign, the subsequent ODE flow will cross the $\dot{y} = 0$ switching manifold at most once. If it does, then the number of zero crossings per delay remains constant because one crossing is removed from the state vector at the instant the delayed feedback switches sign and one zero-crossing is subsequently added. A preserved number of zero crossings allows for the existence of rapidly oscillating periodic solutions. If the ODE flow does not cross the switching manifold, then the number of zero crossing decreases. Importantly, the number of zero-crossings can not increase. This fact sets limits on the possible evolution of the system and is reminiscent of the arguments used to prove facts about the simple behavior of first-order delayed relay systems [11, 12].

In contrast, if DDE (6) is tuned to operate in the underdamped regime, then the number of zero crossings may increase. Accordingly, much richer dynamics and bifurcations are found, including non-standard bifurcations, so-called discontinuity induced bifurcations [20]. In light of this, DDE (6) can be viewed as a system that is intermediary between simple first-order delayed relay systems and general DDEs with their, typically, complex dynamics.

7 Acknowledgements

The project was supported in part by the Reed College Summer Research Fellowship (K.B.) and the Irish Research Council and McAfee LLC under award number EBPPG/2018/269 (R.P.).

A Appendix: Experimental Setup

Shown in Fig. 7 is a circuit schematic of the experimental setup that implements the bandpass filtered time-delayed relay sytem.

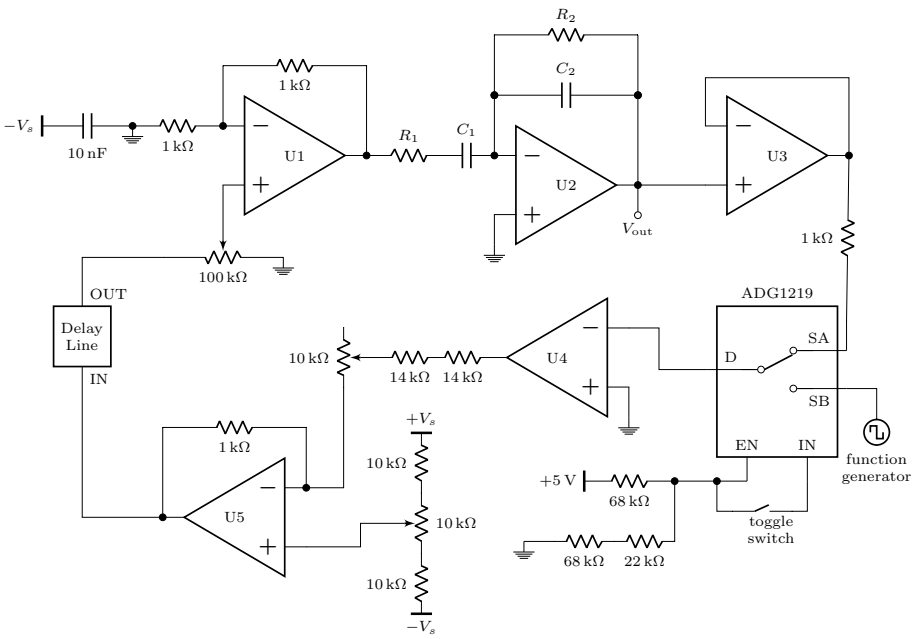

Fig. 7. Circuit diagram in feedback mode (displayed). When the ADG1219 is switched to SB, the circuit is open-loop and driven by a signal from a function generator.

The voltage produced by the amplifier (U1) is fed into a bandpass filter (U2), which produces an output, labelled V_{out}. This signal passes through a buffer (U3) to an ADG1219 analog Single-Pole-Double-Throw (SPDT) switch. The purpose of buffer (U3) and the following resistor is to keep the input current flowing into the switch at safe levels. The ADG1219 is used for fast switching operations between the feedback loop (SA) and an Agilent 33210A arbitrary waveform generator (SB) that is utilized to set the initial history function.

The output of the switch is fed into an operational amplifier acting as an inverting comparator (U4). When the input at the inverting pin is greater than 0, the comparator outputs the negative rail voltage of $-15\,\text{V}$, and vice versa. To be compatible with the input requirements of the delay circuit, the voltage signal is then attenuated, inverted, and offset by an operational amplifier (U5), before being fed into the delay. On the other side of the delay, the signal is amplified using a variable-gain amplifier (U1) with greater than unity gain. The comparator, attenuator, and amplifier (U4, U5, and U1) work in concert to generate the time-delayed relay signal.

The circuit implementing the adjustable delay is based around a First-In-First-Out (FIFO) memory chip sandwiched between an analog-to-digital and a digital-to-analog converter (see [18] for details on a similar circuit). The FIFO-based delay circuit has an input that is limited to a signal of $\pm 1\,\text{V}$ and it generates a small offset on the order of tens of millivolts. To account for these operational limitations, the signal sent into the delay is first attenuated by the variable-gain amplifier (U5) and an adjustable offset is added to cancel the

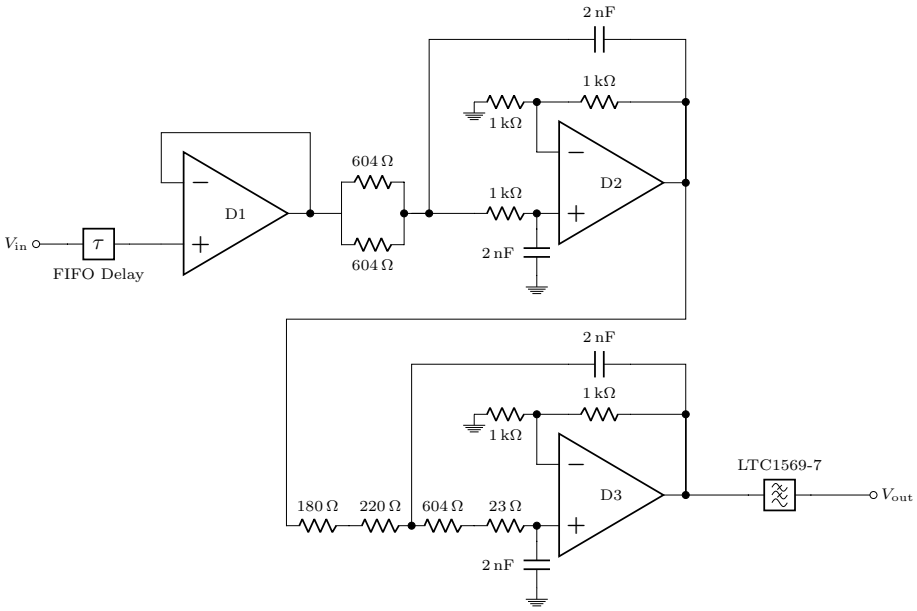

Fig. 8. Filters used to condition the output of the FIFO delay circuit: The delay (τ) is followed by a buffer-follower (D1), a 4th-order lowpass filter (D2 and D3), and a 10th-order lowpass filter (LTC1569-7). Bypass capacitors are not depicted.

delay circuit offset. The delay circuit output, as measured at the buffer-follower (D1) (see Fig. 8), contains some residual high-frequency digital noise. This noise is subsequently filtered out using two low-pass filters: a 4th-order filter built from operational amplifiers D2 and D3, and a 10th-order filter created using an LTC1569-7 integrated circuit. The resulting low-pass filter has a 3dB frequency of 120 kHz, which means that its passband extends to frequencies well above the passband of the bandpass filter in the feedback loop. Therefore, this lowpass filter has no effect on the dynamics, it just serves to suppress noise.

Bandpass filter transfer function: The active bandpass filter in the feedback loop (see U2 in Fig. 7) is a two-pole filter with a transfer function H that, in terms of angular frequency ω, is given by

$$H(\omega) = \frac{\hat{V}_{\text{out}}(\omega)}{\hat{V}_{\text{in}}(\omega)} = -\frac{G}{1 + iQ\left(\omega/\omega_c - \omega_c/\omega\right)}. \tag{8}$$

Here, we introduced the filter center frequency $\omega_c = \sqrt{\omega_1\omega_2}$, in which $\omega_1 = 1/R_1C_1$ and $\omega_2 = 1/R_2C_2$. The filter gain is

$$G = \frac{R_2C_1\omega_1\omega_2}{\omega_1 + \omega_2}$$

and the quality factor, the fraction of filter center frequency and width, is

$$Q = \frac{\sqrt{\omega_1\omega_2}}{\omega_1 + \omega_2}.$$

Hence, one can write

$$\left(1 + iQ(\frac{\omega}{\omega_c} - \frac{\omega_c}{\omega})\right) \hat{V}_{\rm out}(\omega) = -G\,\hat{V}_{\rm in}(\omega), \tag{9}$$

or equivalently, after Laplace transform to the time domain,

$$V_{\rm out}(t) + \frac{Q}{\omega_c}\,\dot{V}_{\rm out}(t) + Q\omega_c \int^t V_{\rm out}(s)\,{\rm d}s = -G\,V_{\rm in}(t). \tag{10}$$

In the experiment, the bandpass filter's upper and lower 3dB frequencies were changed by choosing different values for the resistors R_1 and R_2 (see U2 in Fig. 7) with values given in Tab. 1.

Table 1. Resistance values for the trials performed. Capacitor values of $C_1 = 10.011(7)\,{\rm nF}$ and $C_2 = 31.12(1)\,{\rm nF}$ were used throughout.

Trial	1	2	3	4	5
R_1 (kΩ)	9.88(5)	19.93(1)	4.749(1)	9.88(5)	9.88(5)
R_2 (kΩ)	99.7(5)	99.7(5)	99.7(5)	202.59(2)	50.09(1)

Bibliography

[1] D. A. W. Barton, B. Krauskopf, and R. E. Wilson, "Periodic solutions and their bifurcations in a non-smooth second-order delay differential equation," Dyn. Syst. **21**, 289–311 (2006).

[2] P. Ryan, A. Keane, and A. Amann, "Border-collision bifurcations in a driven time-delay system," Chaos **30**, 023121 (2020).

[3] O. Diekmann, S. A. van Gils, S. V. Lunel, and H.-O. Walther, *Delay Equations*, Applied Mathematical Sciences (Springer New York, NY, 1995).

[4] J. Hale, L. T. Magalhães, and W. L. Oliva, *Dynamics in Infinite Dimensions*, vol. 47 of *Applied mathematical sciences* (Springer-Verlag, New York, 2002), 2nd ed.

[5] T. Erneux, *Applied Delay Differential Equations*, vol. 3 of *Surveys and Tutorials in the Applied Mathematical Sciences* (Springer, 2009).

[6] Y. K. Chembo, D. Brunner, M. Jacquot, and L. Larger, "Optoelectronic oscillators with time-delayed feedback," Rev. Mod. Phys. **91**, 035006 (2019).

[7] T. Heil, I. Fischer, W. Elsässer, J. Mulet, and C. R. Mirasso, "Chaos synchronization and spontaneous symmetry-breaking in symmetrically delay-coupled semiconductor lasers," Phys. Rev. Lett. **86**, 795 (2001).

[8] L. Illing and D. J. Gauthier, "Ultra-high-frequency chaos in a time-delay electronic device with band-limited feedback," Chaos **16**, 033119 (2006).

[9] A. Keane, B. Krauskopf, and C. Postlethwaite, "Delayed feedback versus seasonal forcing: Resonance phenomena in an El Niño Southern Oscillation model," SIAM J. Appl. Dyn. Syst. **14**, 1229 (2015).

[10] A. Keane, B. Krauskopf, and C. Postlethwaite, "Investigating irregular behavior in a model for the El Niño Southern Oscillation with positive and negative delayed feedback," SIAM J. Appl. Dyn. Syst. **15**, 1656 (2016).

[11] E. Fridman, L. Fridman, and E. Shustin, "Steady modes in relay control systems with time delay and periodic disturbances," J. Dyn. Syst. Meas. Control **122**, 732–737 (2000).

[12] E. Fridman, L. Fridman, and E. Shustin, *Sliding Mode Control in Engineering* (Marcel Dekker, New York, 2002), chap. Steady modes in relay systems with delay, pp. 263–293.

[13] E. Shustin, E. Fridman, and L. Fridman, "Oscilltions in a second-order discontinuous system with delay," Discrete Contin. Dyn. Syst. **9**, 339–358 (2003).

[14] L. Benadero, A. E. Aroudi, and E. Ponce, "Delay effects on the limit cycling behavior in resonant inverters with state feedback," Nonlinear Theory Appl. IEICE **10**, 337–356 (2019).

[15] J. Sieber, "Dynamics of delayed relay systems," Nonlinearity **19**, 2489–2527 (2006).

[16] A. N. Sharkovsky, Y. L. Maistrenko, and E. Y. Romanenko, *Difference Equations and their Applications* ((Russian) Nauka Dumka, Kiev 1986; (English) Kluwer, 1993).

[17] M. Akian and P.-A. Bliman, "On Super-high Frequencies in Discontinuous 1st-Order Delay–Differential Equations," J. Differential Equations **162**, 326-358 (2000).
[18] E. Perez, C. Werkheiser, A. Striff, and L. Illing, "Exploring delay dynamics with a programmable electronic delay circuit," Am. J. Phys. **88**, 1006 (2020).
[19] L. Weicker, T. Erneux, D. P. Rosin, and D. J. Gauthier, "Multirhythmicity in an optoelectronic oscillator with large delay," Phys. Rev. E **91**, 012910 (2015).
[20] L. Illing, P. Ryan, and A. Amann, "Dynamics of a time-delayed relay system," arXiv:2306.06498 (2023).